Available online at www.sciencedirect.com
SCIENCE DIRECT®
Applied Mathematical Modelling 29 (2005) 235–252
APPLIED MATHEMATICAL MODELLING
www.elsevier.com/locate/apm

Formulation of hybrid Trefftz finite element method for elastoplasticity

Qing-Hua Qin *

Department of Engineering, Faculty of Engineering and Information Technology, Australian National University, Engineering Building 32, North Road, Canberra, ACT 0200, Australia

Received 1 July 2003; received in revised form 1 August 2004; accepted 6 September 2004

Abstract

The present investigation provides a hybrid Trefftz finite element approach for analysing elastoplastic problems. A dual variational functional is constructed and used to derive hybrid Trefftz finite element formulation for elastoplasticity of bulky solids. The formulation is applicable to either strain hardening or elastic-perfectly plastic materials. A solution algorithm based on initial stress formulation is introduced into the new element model. The performance of the proposed element model is assessed by three examples and comparison is made with results obtained by other approaches. The hybrid Trefftz finite element approach is demonstrated to be particularly suited for nonlinear analysis of two-dimensional elastoplastic problems.

Keywords: Trefftz method; Finite element method; Elastoplasticity

1. Introduction

The hybrid Trefftz (HT) finite element (FE) model, originating about 25 years ago [1,2], has been considerably improved and has now become a highly efficient computational tool for the

* Tel.: +61 2 6125 8274; fax: +61 2 6125 0506.
E-mail address: qinghua.qin@anu.edu.au

0307-904X/$ - see front matter
doi:10.1016/j.apm.2004.09.004

solution of complex boundary value problems. In contrast to conventional FE models, the class of finite elements associated with the Trefftz method is based on a hybrid method which includes the use of an auxiliary inter-element displacement or traction frame to link the internal displacement fields of the elements. Such internal fields, chosen so as to a priori satisfy the governing differential equations, have conveniently been represented as the sum of a particular integral of nonhomogeneous equations and a suitably truncated Trefftz-complete set of regular homogeneous solutions multiplied by undetermined coefficients. Inter-element continuity is enforced by using a modified variational principle together with an independent frame field defined on each element boundary. The element formulation, during which the internal parameters are eliminated at the element level, leads in the end to the standard force-displacement relationship, with a symmetric positive definite stiffness matrix. Clearly, while the conventional FE formulation may be assimilated to a particular form of the Rayleigh–Ritz method, the HT FE approach has a close relationship with the Trefftz method [3]. As noted in [4], the main advantages stemming from the HT FE model are (a) the formulation calls for integration along the element boundaries only, which enables arbitrary polygonal or even curve-sided elements to be generated. As a result, it may be considered as a special, symmetric, substructure-oriented boundary solution (BS) approach, and thus possesses the advantages of the boundary element method (BEM) [4]. In contrast to conventional boundary element formulation, however, the HT FE model avoids the introduction of singular integral equations and does not require the construction of a fundamental solution, which may be very laborious to build; (b) the HT FE model is likely to represent the optimal expansion bases for hybrid-type elements where inter-element continuity need not be satisfied, a priori, which is particularly important for generating a quasi-conforming plate-bending element; (c) the model offers the attractive possibility of developing accurate crack-singular, corner or perforated elements, simply by using appropriate known local solution functions as the trial functions of the intra-element displacements.

The first attempt to generate a general-purpose HT FE formulation occurred in the study by Jirousek and Leon [1] of the effect of mesh distortion on thin plate elements. It was immediately noticed that Trefftz-complete functions represented an optimal expansion basis for hybrid-type elements where inter-element continuity need not be satisfied a priori. Since then, the Trefftz-element concept has become increasingly popular, attracting a growing number of researchers into this field [4,5]. Trefftz elements have been successfully applied to problems of elasticity [6], Kirchhoff plates [7,8], moderately thick Reissner–Mindlin plates [9], thick plates [10], general three-dimensional solid mechanics [10,11], axisymmetric solid mechanics [12], potential problems [13,14], shells [15], elastodynamic problems [16,17], transient heat conduction analysis [18], and geometrically nonlinear plate bending [19]. Although remarkable progress has been made in developing HT FE formulation for analyzing linear elastic problems, comparatively little progress has been made in applications of HT FE formulation to materially nonlinear problems. The earliest Trefftz formulation for elastoplasticity appears to be due to Zielinski [20]. He applied a globally based Trefftz-type method to plasticity, in which the fundamental solutions with singularities outside the given area were used as shape functions and the iterative algorithm was based on the initial stress approach. Freitas and Wang [21] presented a stress model of Trefftz-elements (or T-elements for short) for analyzing quasi-static, gradient-dependent elastoplasticity problems. The FE approximation consists of direct estimation of the stress and plastic multiplier fields in the domain of the element as well as of the displacements and plastic multiplier gradients on its

boundary. In their analysis, the model is assumed to be of geometrically linear response. The elastoplastic constitutive relations are uncoupled into elastic and plastic deformation modes. The present paper reports development of a new HT FE model which seems to be suitable for practical engineering analysis and is easy to implement into standard FE computer programming code. A pair of dual variational functionals is presented and used to derive the corresponding HT FE formulation of elastoplastic materials. The formulation is applicable to strain hardening and elastic-perfectly plastic materials. The corresponding yield criteria of these materials and the initial stress scheme are employed to calculate the so-called plastic stresses and strains. Three numerical example are considered to demonstrate the efficiency of the proposed element formulation in nonlinear analysis of elastoplasticity problems.

2. Basic governing equations of elastoplasticity

Consider an elastoplastic solid, occupying a two-dimensional arbitrary shaped domain Ω bounded by its boundary Γ. Throughout this paper, repeated indices i, j and k imply the summation convention of Einstein. In the "small" deformation range, compatibility and equilibrium are expressed in the incremental form

$$\dot{\boldsymbol{\sigma}}_{ij,j} + \dot{b}_i = 0 \quad \text{in } \Omega, \tag{1}$$

$$\dot{\varepsilon}_{ij} = \frac{1}{2}(\dot{u}_{i,j} + \dot{u}_{j,i}) \quad \text{in } \Omega, \tag{2}$$

$$\dot{u}_i = \dot{\bar{u}}_i \quad \text{on } \Gamma_u, \tag{3}$$

$$\dot{t}_i = \dot{\boldsymbol{\sigma}}_{ij} n_j = \dot{\bar{t}}_i \quad \text{on } \Gamma_{\boldsymbol{\sigma}}, \tag{4}$$

where the dot indicates an increment, $\dot{\boldsymbol{\sigma}}_{ij}$ and $\dot{\varepsilon}_{ij}$ are stresses and strains, $\dot{b}_i$ body forces, $\dot{u}_i$ displacements, $\dot{\bar{u}}_i$ and $\dot{\bar{p}}_j$ prescribed boundary displacements and tractions, Γ_u and $\Gamma_{\boldsymbol{\sigma}}$ the constrained and free parts of the boundary Γ, n_i the direction cosines of the outward normal to Γ, uniquely defined everywhere since Γ will be assumed to be smooth, for simplicity. The strain $\dot{\varepsilon}_{ij}$ may be decomposed into its elastic and plastic parts:

$$\dot{\varepsilon}_{ij} = \dot{\varepsilon}^{\mathrm{e}}_{ij} + \dot{\varepsilon}^{\mathrm{p}}_{ij}. \tag{5}$$

With expression (5), the stress strain equation can be written as

$$\dot{\boldsymbol{\sigma}}_{ij} = \lambda\delta_{ij}(\dot{\varepsilon}_{kk} - \dot{\varepsilon}^{\mathrm{p}}_{kk}) + 2G(\dot{\varepsilon}_{ij} - \dot{\varepsilon}^{\mathrm{p}}_{ij}) = \dot{\boldsymbol{\sigma}}^{\mathrm{e}}_{ij} + \dot{\boldsymbol{\sigma}}^{\mathrm{p}}_{ij}, \tag{6}$$

where $\delta_{ij} = 1$ for $i = j$ and 0 for $i \neq j$ and $\dot{\boldsymbol{\sigma}}^{\mathrm{e}}_{ij}$, $\dot{\boldsymbol{\sigma}}^{\mathrm{p}}_{ij}$, G are defined by

$$\dot{\boldsymbol{\sigma}}^{\mathrm{e}}_{ij} = \frac{E}{3(1-2v)}\delta_{ij}\dot{\varepsilon}_{kk} + 2G\dot{\varepsilon}_{ij}, \quad \dot{\boldsymbol{\sigma}}^{\mathrm{p}}_{ij} = -\frac{E}{3(1-2v)}\delta_{ij}\dot{\varepsilon}^{\mathrm{p}}_{kk} - 2G\dot{\varepsilon}^{\mathrm{p}}_{ij}, \quad G = \frac{E}{2(1+v)} \tag{7}$$

with E and v being Young's modulus and Poisson's ratio.

Substituting Eq. (6) into (1) and using Eqs. (2) and (5), the governing differential equation (1) can be rewritten as [22]

$$G\dot{u}_{i,jj} + (\lambda + G)\dot{u}_{j,ij} + \dot{b}_i^{\mathrm{ep}} = 0 \quad \text{in } \Omega \tag{8}$$

and the natural boundary (4) is replaced by

$$\dot{t}_{i0} = \dot{\boldsymbol{\sigma}}_{ij}^{\mathrm{e}} n_j = (\dot{\boldsymbol{\sigma}}_{ij} - \dot{\boldsymbol{\sigma}}_{ij}^{\mathrm{p}}) n_j = \dot{\bar{t}}_i - \dot{\boldsymbol{\sigma}}_{ij}^{\mathrm{p}} n_j = \dot{\bar{t}}_{i0}, \tag{9}$$

where $\dot{b}_i^{\mathrm{ep}} = \dot{b}_i + \dot{\boldsymbol{\sigma}}_{ij,j}^{\mathrm{p}}$. The plastic part of stresses $\dot{\boldsymbol{\sigma}}_{ij}^{\mathrm{p}}$ is described in Appendix A.

Moreover, in the Trefftz FE approach, Eqs. (1)–(9) should be completed by adding the following inter-element continuity requirements:

$$\dot{u}_{ie} = \dot{u}_{if} \quad (\text{on } \Gamma_e \cap \Gamma_f, \text{ conformity}), \tag{10}$$

$$(\dot{\boldsymbol{\sigma}}_{ij} n_j)_e + (\dot{\boldsymbol{\sigma}}_{ij} n_j)_f = 0 \quad (\text{on } \Gamma_e \cap \Gamma_f, \text{ reciprocity}), \tag{11}$$

where 'e' and 'f' stand for any two neighbouring elements. Eqs. (1)–(11) are taken as a basis to establish the modified variational principle for Trefftz FE analysis in elastoplasticity.

3. Modified variational principles

The Trefftz FE equation for an elastic solid can be established by the variational approach [5]. Since the stationary conditions of the traditional potential and complementary variational functional cannot guarantee the satisfaction of the inter-element continuity condition which is required in the Trefftz FE analysis, some new variational functionals need to be developed. Piltner [23] presented two different variational formulations to treat special elements with holes or cracks. The formulation consists of a conventional potential energy and a least square functional. The least square functional was not added as a penalty function to the potential functional, but is minimized separately for the special elements considered. Jirousek [24] developed a variational functional in which either the displacement conformity or the reciprocity of the conjugate tractions is enforced at the element interfaces. Jirousek and Zielinski [25] obtained two complementary HT formulations based on weighted residual method. The dual formulations enforced the reciprocity of boundary tractions more strongly than the conformity of the displacement fields. Qin [5] presented a modified variational principle based on HT displacement frame. The variational functional of Qin [5] is, however, limited to the case that nodes containing unknown displacements must connect with at least one inter-element boundary. To remove this limitation, we present a pair of dual variational functionals based on the total potential energy and complementary energy as

$$\Pi_m = \sum_e \Pi_{me} = \sum_e \left\{ \Pi_e + \int_{\Gamma_{te}} (\dot{\bar{t}}_{i0} - \dot{t}_i)\dot{\tilde{u}}_i \,\mathrm{d}s - \int_{\Gamma_{Ie}} \dot{\boldsymbol{\sigma}}_{ij} n_j \dot{\tilde{u}}_i \,\mathrm{d}s \right\}, \tag{12a}$$

$$\Psi_m = \sum_e \Psi_{me} = \sum_e \left\{ \Psi_e + \int_{\Gamma_{ue}} (\dot{\bar{u}}_i - \dot{u}_i)\dot{\sigma}_{ij} n_j \, \mathrm{d}s - \int_{\Gamma_{Ie}} \dot{\sigma}_{ij} n_j \dot{\bar{u}}_i \, \mathrm{d}s \right\}, \tag{12b}$$

where

$$\Pi_e = \iint_{\Omega_e} \Pi(\dot{\sigma}_{ij}) \, \mathrm{d}\Omega - \int_{\Gamma_{ue}} \dot{\sigma}_{ij} n_j \dot{\bar{u}}_i \, \mathrm{d}s, \tag{13a}$$

$$\Psi_e = \iint_{\Omega_e} (\Psi(\dot{\varepsilon}_{ij}) - \dot{b}_i \dot{u}_i) \, \mathrm{d}\Omega - \int_{\Gamma_{te}} \dot{\bar{t}}_i \dot{\bar{u}}_i \, \mathrm{d}s, \tag{13b}$$

with [27]

$$\Pi(\dot{\sigma}_{ij}) = \frac{1-2v}{6E} (\dot{\sigma}_{ii})^2 + \frac{\dot{\sigma}_{ij}\dot{\sigma}_{ij}}{4G} - \frac{1}{2}\alpha^{**} h\dot{f}^2, \tag{14a}$$

$$\Psi(\dot{\varepsilon}_{ij}) = \frac{E}{6(1-2v)} (\dot{\varepsilon}_{ii})^2 + G\dot{e}_{ij}\dot{e}_{ij} - \alpha^* \frac{G\left(\dfrac{\partial f}{\partial \sigma_{kl}} \dot{\varepsilon}_{kl}\right)^2}{\left(\dfrac{1}{2Gh} + \dfrac{\partial f}{\partial \sigma_{pq}} \dfrac{\partial f}{\partial \sigma_{pq}}\right)} \tag{14b}$$

in which Eq. (8) is assumed to be satisfied, a priori, $\alpha^*, \alpha^{**}, \dot{e}_{ij}, f$ and h are defined in Appendix A. The terminology "modified principle" refers, here, to the use of a conventional functional (Π_e or Ψ_e here) and some modified terms for the construction of a special variational principle to account for additional requirements such as the condition defined in Eqs. (10) and (11).

The boundary Γ_e of a particular element consists of the following parts:

$$\Gamma_e = \Gamma_{ue} \cup \Gamma_{te} \cup \Gamma_{Ie}, \tag{15}$$

where

$$\Gamma_{ue} = \Gamma_u \cap \Gamma_e, \quad \Gamma_{te} = \Gamma_t \cap \Gamma_e \tag{16}$$

and Γ_{Ie} is the inter-element boundary of the element 'e'. We now show that the stationary condition of the functional (12a) [or (12b)] leads to Eqs. (3), (4), (10), (11), and ($\dot{u}_i = \dot{\bar{u}}_i$ on Γ_t), and present the theorem on the existence of extremum of the functional, which ensures that an approximate solution can converge to the exact one. Taking Π_m as an example, we have the following two statements:

(a) *Modified complementary principle*

$$\delta\Pi_m = 0 \Rightarrow (3), (4), (10), (11) \text{ and } (\dot{u}_i = \dot{\bar{u}}_i \text{ on } \Gamma_t), \tag{17}$$

where δ stands for the variation symbol.

(b) *Theorem on the existence of extremum*

If the expression

$$\iint_{\Omega} \delta^2 \Pi(\dot{\sigma}_{ij}) \, \mathrm{d}\Omega - \int_{\Gamma_t} \delta\dot{t}_i \delta\dot{\bar{u}}_i \, \mathrm{d}s - \sum_e \int_{\Gamma_{eI}} \delta\dot{\bar{u}}_i \delta\dot{\sigma}_{ij} n_j \, \mathrm{d}s \tag{18}$$

is uniformly positive (or negative) in the neighborhood of u_{i0}, where the displacement u_{i0} has such a value that $\Pi_m(u_{i0}) = (\Pi_m)_0$, and where $(\Pi_m)_0$ stands for the stationary value of Π_m, we have

$$\Pi_m \geqslant (\Pi_m)_0 \quad [\text{or } \Pi_m \leqslant (\Pi_m)_0] \tag{19}$$

in which the relation that $\tilde{u}_{ie} = \tilde{u}_{if}$ is identical on $\Gamma_e \cap \Gamma_f$ has been used. This is due to the definition in Eq. (31) of Section 4.

Proof: First, we derive the stationary conditions of functional (12a). To this end, performing a variation of Π_m and noting that Eq. (1) holds true a priori by the previous assumption, we obtain

$$\begin{aligned}\delta\Pi_m = &\int_{\Gamma_u} (\dot{u}_i - \dot{\tilde{u}}_i)\delta\dot{\boldsymbol{\sigma}}_{ij} n_j \,\mathrm{d}s + \int_{\Gamma_t} ((\dot{\bar{t}}_i - \dot{t}_i)\delta\dot{\tilde{u}}_i + (\dot{u}_i - \dot{\tilde{u}}_i)\delta\dot{t}_i)\,\mathrm{d}s \\ &+ \sum_e \int_{\Gamma_{el}} [(\dot{u}_i - \dot{\tilde{u}}_i)\delta\dot{\boldsymbol{\sigma}}_{ij} n_j - \dot{\boldsymbol{\sigma}}_{ij} n_j \delta\dot{\tilde{u}}_i]\,\mathrm{d}s.\end{aligned} \tag{20}$$

Therefore, the Euler equations for expression (20) are Eqs. (3), (4), (10), (11) and $u_i = \tilde{u}_i$ on Γ_t as the quantities $\delta t_i, \delta\dot{\boldsymbol{\sigma}}_{ij}, \delta u_i$ and $\delta\tilde{u}_i$ may be arbitrary. The principle (17) has thus been proved. This indicates that the stationary condition of the functional satisfies the required boundary and inter-element continuity equations and can thus be used for deriving Trefftz FE formulation.

As for the proof of the theorem on the existence of extremum, we may complete it by way of the so-called "second variational approach" [26]. In doing this, performing variation of $\delta\Pi_m$ and using the constrained conditions (8), we find

$$\delta^2\Pi_m = \iint_\Omega \delta^2\Pi(\dot{\boldsymbol{\sigma}}_{ij})\,\mathrm{d}\Omega - \int_{\Gamma_t} \delta\dot{t}_i \delta\dot{\tilde{u}}_i \,\mathrm{d}s - \sum_e \int_{\Gamma_{el}} \delta\dot{\tilde{u}}_i \delta\dot{\boldsymbol{\sigma}}_{ij} n_j \,\mathrm{d}s = \text{expression (18)}. \tag{21}$$

Therefore the theorem has been proved from the sufficient condition of the existence of a local extreme of a functional [26]. This completes the proof. The function Ψ_m can be stated and proved similarly. We omit those details for the sake of conciseness.

4. Assumed fields

The main idea of the Trefftz FE approach is to establish a FE formulation whereby intra-element continuity is enforced on a nonconforming internal displacement field chosen so as to a priori satisfy the governing differential equation of the problem under consideration [5]. In other words, as an obvious alternative to the Rayleigh–Ritz method as a basis for a FE formulation, the model, here, is based on the method of Trefftz [3]. With this method the solution domain Ω is subdivided into elements, and over each element 'e' the assumed intra-element fields (for a two-dimensional problem) are

$$\dot{\mathbf{u}} = \begin{Bmatrix} \dot{u}_1 \\ \dot{u}_2 \end{Bmatrix} = \dot{\breve{\mathbf{u}}} + \sum_{i=1}^{m} \mathbf{N}_i \dot{\mathbf{c}}_i = \dot{\breve{\mathbf{u}}} + \mathbf{N}\dot{\mathbf{c}}, \tag{22}$$

where $\dot{\mathbf{c}}_i$ stands for undetermined coefficient, and $\dot{\breve{\mathbf{u}}}(=\{\dot{\breve{u}}_1 \quad \dot{\breve{u}}_2\}^{\mathrm{T}})$ and $\mathbf{N}_i$ are known functions. If the governing differential equation (8) is rewritten in a general form

$$\mathfrak{R}\dot{\mathbf{u}}(\mathbf{x}) + \dot{\mathbf{b}}^{\mathrm{ep}}(\mathbf{x}) = 0 \quad (\mathbf{x} \in \Omega_e), \tag{23}$$

where $\mathfrak{R}$ stands for the differential operator matrix for Eq. (8), $\mathbf{x}$ for position vector, $\dot{\mathbf{b}}^{\mathrm{ep}}(=\{\dot{b}_1^{\mathrm{ep}} \quad \dot{b}_2^{\mathrm{ep}}\}^{\mathrm{T}})$ for the known right-hand term, and Ω_e stands for the subdomain of the eth element, then $\dot{\breve{\mathbf{u}}} = \dot{\breve{\mathbf{u}}}(\mathbf{x})$ and $\mathbf{N}_i = \mathbf{N}_i(\mathbf{x})$ in Eq. (22) must be chosen such that

$$\mathfrak{R}\,\dot{\breve{\mathbf{u}}} + \dot{\mathbf{b}}^{\mathrm{ep}} = 0 \text{ and } \mathfrak{R}\mathbf{N}_i = 0 \quad (i = 1, 2, \ldots, m) \tag{24}$$

everywhere in Ω_e. A complete system of homogeneous solutions $\mathbf{N}_i$ can be generated in a systematic way from Muskhelishvili's complex variable formulation [6]. For convenience, we list the results presented in [6] as follows:

$$2G\mathbf{N}_j = \begin{Bmatrix} \mathrm{Re}\, Z_{1k} \\ \mathrm{Im}\, Z_{1k} \end{Bmatrix} \quad \text{with } Z_{1k} = \mathrm{i}\kappa z^k + k\mathrm{i}z\bar{z}^{k-1}, \tag{25}$$

$$2G\mathbf{N}_{j+1} = \begin{Bmatrix} \mathrm{Re}\, Z_{2k} \\ \mathrm{Im}\, Z_{2k} \end{Bmatrix} \quad \text{with } Z_{2k} = \kappa z^k - kz\bar{z}^{k-1}, \tag{26}$$

$$2G\mathbf{N}_{j+2} = \begin{Bmatrix} \mathrm{Re}\, Z_{3k} \\ \mathrm{Im}\, Z_{3k} \end{Bmatrix} \quad \text{with } Z_{3k} = \mathrm{i}\bar{z}^k, \tag{27}$$

$$2G\mathbf{N}_{j+3} = \begin{Bmatrix} \mathrm{Re}\, Z_{4k} \\ \mathrm{Im}\, Z_{4k} \end{Bmatrix} \quad \text{with } Z_{4k} = -\bar{z}^k, \tag{28}$$

where $z = x + \mathrm{i}y$ and $\mathrm{i} = \sqrt{-1}$.

The particular solution $\dot{\breve{\mathbf{u}}}$ can be obtained by means of its source function. The source function corresponding to Eq. (8) has been given in [28] as

$$u_{ij}^*(r_{pq}) = \frac{1+\nu}{4\pi E}[-(3-\nu)\delta_{ij}\ln r_{pq} + (1+\nu)r_{pq,i}r_{pq,j}], \tag{29}$$

where $r_{pq} = [(x_q - x_p)^2 + (y_q - y_p)^2]^{1/2}$, $u_{ij}^*(r_{pq})$ denotes ith component of displacement at the field point q of the solid under consideration when a unit point force is applied in the jth direction at the source point p. Using this source function, the particular solution can be expressed by

$$\dot{\breve{\mathbf{u}}} = \begin{Bmatrix} \dot{\breve{u}}_1 \\ \dot{\breve{u}}_2 \end{Bmatrix} = \int\!\!\int_{\Omega} \dot{b}_j^{\mathrm{ep}} \begin{Bmatrix} u_{1j}^* \\ u_{2j}^* \end{Bmatrix} \mathrm{d}\Omega. \tag{30}$$

The unknown coefficient $\dot{\mathbf{c}}$ may be calculated from conditions on the external boundary and/or the continuity conditions on the inter-element boundary. Thus various Trefftz element models

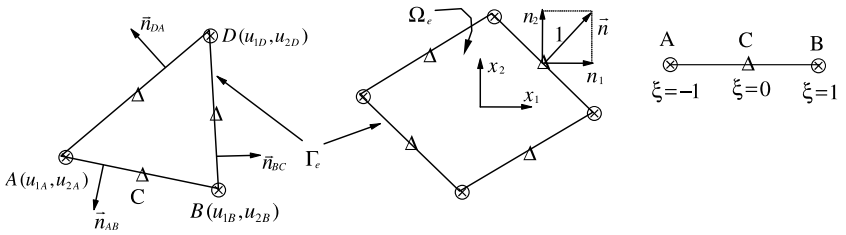

Fig. 1. Trefftz element in plane problem.

can be obtained by using different approaches to enforce these conditions. In the majority of them a hybrid technique is used, whereby the elements are linked through an auxiliary conforming displacement frame which has the same form as in conventional FE method. This means that in the Trefftz FE approach, a conforming displacement field should be independently defined on the element boundary to enforce the field continuity between elements and also to link the coefficient $\dot{\mathbf{c}}$, appearing in Eq. (22), with nodal displacement $\dot{\mathbf{d}}$. The frame is defined as

$$\dot{\tilde{\mathbf{u}}}(\mathbf{x}) = \widetilde{\mathbf{N}}(\mathbf{x})\dot{\mathbf{d}} \quad (\mathbf{x} \in \Gamma_e), \tag{31}$$

where the symbol "$\sim$" is used to specify that the field is defined on the element boundary only, $\dot{\mathbf{d}} = \dot{\mathbf{d}}(\dot{\mathbf{c}})$ stands for the vector of the nodal displacements which are the final unknowns of the finite element formulation, Γ_e represents the boundary of element e, and $\widetilde{\mathbf{N}}$ is a matrix of the corresponding shape functions which are the same as those in conventional FE formulation. For example, along the side A–B of a particular element (see Fig. 1), a simple interpolation of the frame displacements may be given in the form

$$\dot{\tilde{\mathbf{u}}}_{\mathrm{AB}} = \begin{Bmatrix} \dot{\tilde{u}}_1 \\ \dot{\tilde{u}}_2 \end{Bmatrix} = \frac{1}{2}\begin{bmatrix} 1-\xi & 0 & 1+\xi & 0 \\ 0 & 1-\xi & 0 & 1+\xi \end{bmatrix}\dot{\mathbf{d}}_{\mathrm{AB}}, \tag{32}$$

where $\dot{\mathbf{d}}_{\mathrm{AB}} = \{\, \dot{u}_{1\mathrm{A}} \quad \dot{u}_{2\mathrm{A}} \quad \dot{u}_{1\mathrm{B}} \quad \dot{u}_{2\mathrm{B}} \,\}^{\mathrm{T}}$, and ξ is shown in Fig. 1.

The tractions $\dot{\mathbf{t}} = \{\, \dot{t}_1 \quad \dot{t}_2 \,\}^{\mathrm{T}}$ appearing in Eq. (9) can be derived from Eqs. (2), (6), (9), (22), and denote

$$\dot{\mathbf{t}}_0 = \begin{Bmatrix} \dot{\mathbf{t}}_{10} \\ \dot{\mathbf{t}}_{20} \end{Bmatrix} = \begin{Bmatrix} \dot{\boldsymbol{\sigma}}^{\mathrm{e}}_{1j} n_j \\ \dot{\boldsymbol{\sigma}}^{\mathrm{e}}_{2j} n_j \end{Bmatrix} = \mathbf{Q}\dot{\mathbf{c}} + \breve{\mathbf{T}}. \tag{33}$$

5. Element stiffness matrix

The element matrix equation can be generated by setting $\delta\Pi_{me} = 0$ or $\delta\Psi_{me} = 0$. To simplify the derivation, we first transform all domain integrals in Eq. (12a) into boundary ones. In fact, by reason of solution properties of the intra-element trial functions the functional Π_{me} can be simplified to

$$\Pi_{me} = \frac{1}{2}\int_{\Omega_e} \dot{b}_i \dot{u}_i \,\mathrm{d}\Omega + \frac{1}{2}\int_{\Gamma_e} \dot{t}_{i0}\dot{u}_i \,\mathrm{d}s + \int_{\Gamma_{te}} (\dot{\bar{t}}_{i0} - \dot{t}_{i0})\dot{\tilde{u}}_i \,\mathrm{d}s - \int_{\Gamma_{Ie}} \dot{t}_{i0}\dot{\tilde{u}}_i \,\mathrm{d}s - \int_{\Gamma_{ue}} \dot{t}_{i0}\dot{\bar{u}}_i \,\mathrm{d}s + \frac{1}{2}\int_{\Gamma_e} \dot{\sigma}^{\mathrm{p}}_{ij}\dot{u}_i n_j \,\mathrm{d}s - \int_{\Gamma_{Ie}} \dot{\sigma}^{\mathrm{p}}_{ij}\dot{\tilde{u}}_i n_j \,\mathrm{d}s - \int_{\Gamma_{ue}} \dot{\sigma}^{\mathrm{p}}_{ij}\dot{\bar{u}}_i n_j \,\mathrm{d}s. \tag{34}$$

Substituting the expressions given in Eqs. (22) and (31) into (33) produces

$$\Pi_{me} = \frac{1}{2}\dot{\mathbf{c}}^{\mathrm{T}}\mathbf{H}\dot{\mathbf{c}} + \dot{\mathbf{c}}^{\mathrm{T}}\mathbf{S}\dot{\mathbf{d}} + \dot{\mathbf{c}}^{\mathrm{T}}\mathbf{r}_1 + \dot{\mathbf{d}}^{\mathrm{T}}\mathbf{r}_2 + \text{terms without } \dot{\mathbf{c}} \text{ or } \dot{\mathbf{d}} \tag{35}$$

in which the matrices $\mathbf{H}$, $\mathbf{S}$ and the vectors $\mathbf{r}_1$, $\mathbf{r}_2$ are as follows:

$$\begin{aligned}
\mathbf{H} &= \int_{\Gamma_e} \mathbf{Q}^{\mathrm{T}}\mathbf{N}\,\mathrm{d}s,\\
\mathbf{S} &= -\int_{\Gamma_{te}} \mathbf{Q}^{\mathrm{T}}\widetilde{\mathbf{N}}\,\mathrm{d}s - \int_{\Gamma_{Ie}} \mathbf{Q}^{\mathrm{T}}\widetilde{\mathbf{N}}\,\mathrm{d}s,\\
\mathbf{r}_1 &= \frac{1}{2}\int_{\Omega_e} \mathbf{N}^{\mathrm{T}}\dot{\mathbf{b}}\,\mathrm{d}\Omega + \frac{1}{2}\int_{\Gamma_e} \left[\mathbf{Q}^{\mathrm{T}}\dot{\overset{\cdot}{\mathbf{u}}} + \mathbf{N}^{\mathrm{T}}\left(\dot{\overset{\cdot}{\mathbf{T}}} + \begin{Bmatrix} \dot{\sigma}^{\mathrm{p}}_{1j} n_j \\ \dot{\sigma}^{\mathrm{p}}_{2j} n_j \end{Bmatrix}\right)\right] \mathrm{d}s - \int_{\Gamma_{ue}} \mathbf{Q}^{\mathrm{T}}\dot{\bar{\mathbf{u}}},\\
\mathbf{r}_2 &= \int_{\Gamma_{te}} \widetilde{\mathbf{N}}^{\mathrm{T}}(\dot{\bar{\mathbf{t}}}_0 - \dot{\overset{\cdot}{\mathbf{T}}})\,\mathrm{d}s - \int_{\Gamma_{Ie}} \widetilde{\mathbf{N}}^{\mathrm{T}}\left(\dot{\overset{\cdot}{\mathbf{T}}} + \begin{Bmatrix} \dot{\sigma}^{\mathrm{p}}_{1j} n_{j\cdot} \\ \dot{\sigma}^{\mathrm{p}}_{2j} n_j \end{Bmatrix}\right) \mathrm{d}s,
\end{aligned} \tag{36}$$

where $\dot{\bar{\mathbf{t}}}_0 = \{\dot{\bar{\mathbf{t}}}_{10} \quad \dot{\bar{\mathbf{t}}}_{20}\}^{\mathrm{T}}$ is the prescribed traction vector.

To enforce inter-element continuity on the common element boundary, the unknown vector $\dot{\mathbf{c}}$ should be expressed in terms of nodal DOF $\dot{\mathbf{d}}$. An optional relationship between $\dot{\mathbf{c}}$ and $\dot{\mathbf{d}}$ in the sense of variation can be obtained from

$$\frac{\partial \Pi_{me}}{\partial \dot{\mathbf{c}}^{\mathrm{T}}} = \mathbf{H}\dot{\mathbf{c}} + \mathbf{S}\dot{\mathbf{d}} + \mathbf{r}_1 = 0. \tag{37}$$

This leads to

$$\dot{\mathbf{c}} = -\mathbf{G}\dot{\mathbf{d}} - \mathbf{g}, \tag{38}$$

where $\mathbf{G} = \mathbf{H}^{-1}\mathbf{S}$ and $\mathbf{g} = \mathbf{H}^{-1}\mathbf{r}_1$, and then straightforwardly yields the expression of Π_{me} only in terms of $\dot{\mathbf{d}}$ and other known matrices

$$\Pi_{me} = -\frac{1}{2}\dot{\mathbf{d}}^{\mathrm{T}}\mathbf{G}^{\mathrm{T}}\mathbf{H}\mathbf{G}\dot{\mathbf{d}} + \dot{\mathbf{d}}^{\mathrm{T}}(\mathbf{r}_2 - \mathbf{G}^{\mathrm{T}}\mathbf{r}_1) + \text{terms without } \dot{\mathbf{d}}. \tag{39}$$

Therefore, the element stiffness matrix equation can be obtained by taking the vanishing variation of the functional Π_{me} as

$$\frac{\partial \Pi_{me}}{\partial \dot{\mathbf{d}}^{\mathrm{T}}} = 0 \Rightarrow \mathbf{K}\dot{\mathbf{d}} = \dot{\mathbf{P}} = \dot{\mathbf{P}}_0 + \mathbf{P}(\dot{\sigma}^{\mathrm{p}}_{ij}), \tag{40}$$

where $\mathbf{K} = \mathbf{G}^{\mathrm{T}}\mathbf{H}\mathbf{G}$ and $\mathbf{P} = -\mathbf{G}^{\mathrm{T}}\mathbf{r}_1 + \mathbf{r}_2$ are, respectively, the element stiffness matrix and the equivalent nodal force vector. The expression (40) is the elemental stiffness matrix equation for

Trefftz FE analysis. $\mathbf{K}$ and $\dot{\mathbf{P}}_0$ can be calculated in the usual way, while $\mathbf{P}(\dot{\boldsymbol{\sigma}}_{ij}^{\mathrm{p}})$ contains unknown $\dot{\boldsymbol{\sigma}}_{ij}^{\mathrm{p}}$. An iterative procedure is thus required. The procedure is briefly described in the next section.

6. Iterative scheme

The steps of the iterative procedure are described as follows:

At the first loading step, assume $\mathbf{P}(\dot{\boldsymbol{\sigma}}_{ij}^{\mathrm{p}}) = 0$. Then solve Eq. (40) for $\dot{\mathbf{d}}$ and calculate $\dot{\boldsymbol{\sigma}}_{ij}^{\mathrm{e}}$ and $\dot{\boldsymbol{\sigma}}_{ij}^{\mathrm{p}}$ using Eqs. (A.11) or (A.13) as well as $\mathbf{P}(\dot{\boldsymbol{\sigma}}_{ij}^{\mathrm{p}})$.

Suppose that $\mathbf{d}^{(k)}, \boldsymbol{\sigma}_{ij}^{(k)}$ and $\boldsymbol{\sigma}_{ij}^{p(k)}$ stand for the kth approximations, which can be obtained from the preceding cycle of iteration. The $(k+1)$th solution may be calculated as follows:

(1) Apply a load increment and take $\mathbf{d}^{(k)}, \boldsymbol{\sigma}_{ij}^{(k)}$ and $\boldsymbol{\sigma}_{ij}^{p(k)}$ as initial values.
(2) Enter the iterative cycle for $i = 1, 2, \ldots$ Calculate the stress increments in all elements using the formulation in Appendix A. Calculate the total stress and compile a list of yielded elements. Calculate the correct stresses in the elastoplastic elements by using Eqs. (A.11) or (A.13).
(3) Calculate $\mathbf{P}(\dot{\boldsymbol{\sigma}}_{ij}^{\mathrm{p}})$ in Eq. (40) using the current value of $\dot{\mathbf{d}}^{[i-1]}$ and $\dot{\boldsymbol{\sigma}}_{ij}^{p[i-1]}$, where the superscript $[i-1]$ stands for the increments at the $(i-1)$th iterative cycle. Solve Eq. (40) for $\dot{\mathbf{d}}^{[i]}$.
(4) If $\eta_i = [(\dot{\mathbf{d}}^{[i]})^{\mathrm{T}}\dot{\mathbf{d}}^{[i]} - (\dot{\mathbf{d}}^{[i-1]})^{\mathrm{T}}\dot{\mathbf{d}}^{[i-1]}]/(\dot{\mathbf{d}}^{[i-1]})^{\mathrm{T}}\dot{\mathbf{d}}^{[i-1]} \leqslant \eta$ (η is a convergence tolerance), proceed to the next loading step and calculate

$$\begin{aligned} \mathbf{d}^{(k+1)} &= \mathbf{d}^{(k+1)} + \dot{\mathbf{d}}^{[i]}, \\ \boldsymbol{\sigma}_{ij}^{(k+1)} &= \boldsymbol{\sigma}_{ij}^{(k)} + \dot{\boldsymbol{\sigma}}_{ij}^{[i]}, \\ \boldsymbol{\sigma}_{ij}^{p(k+1)} &= \boldsymbol{\sigma}_{ij}^{p(k)} + \dot{\boldsymbol{\sigma}}_{ij}^{p[i]} \end{aligned} \tag{41}$$

otherwise, go back to step (2).

It is noted that the required stiffness matrices appearing in Eq. (40) do not change through each step of computation. Hence, once the matrix $\mathbf{K}$ has been formed, they can be stored in the core and used in each cycle of iteration without any change. Obviously this can save a large amount of computing time.

7. Numerical applications

Since the main purpose of this paper is to outline the basic principles of the proposed method and demonstrate its feasibility, numerical assessment is limited to an infinitely long thick cylinder under internal pressure, a notched tension specimen, and a perforated strip under tension. In all the computation, the convergence tolerance $\eta = 0.001$ is used.

Example 1. An infinitely long thick cylinder subjected to internal pressure p. In this example, the plane strain expansion of a thick cylinder under internal pressure is studied (see Fig. 2). An elastic-

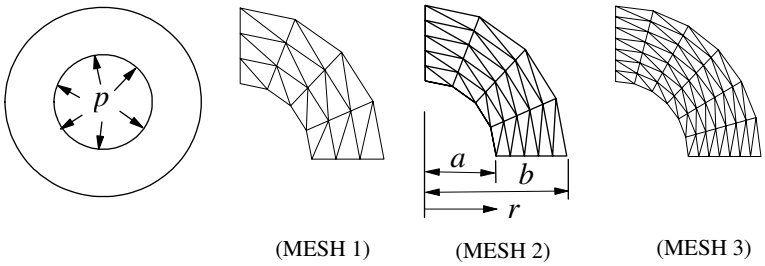

Fig. 2. Mesh and geometry of internally pressured thick cylinder.

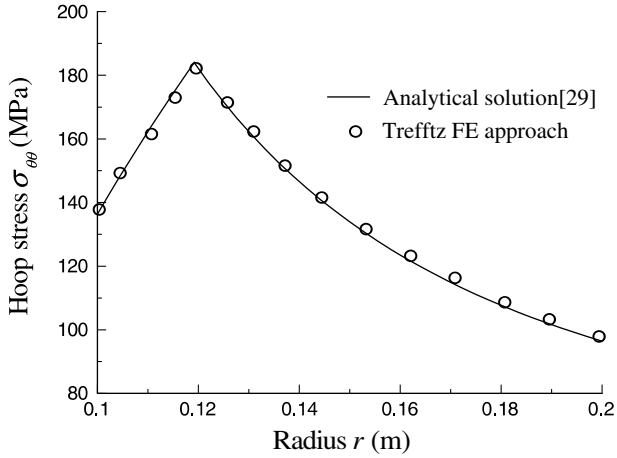

Fig. 3. Hoop stress distributions for the thick cylinder along radius (mesh 2).

perfectly plastic material is assumed with the von Mises yield criterion (i.e., $H' = 0$). The initial parameters used are taken to be $a = 100\,\text{mm}$ $b = 200\,\text{mm}$, $E = 20.58 \times 10^4\,\text{MPa}$, $v = 0.3$, uniaxial yield stress $\sigma_s = 235.2\,\text{MPa}$ and the internal pressure $p = 135.3\,\text{MPa}$. Due to the problem being radially symmetric, one quadrant of the thick cylinder is used in the analysis. The numerical results of stress distributions with mesh 2 (see Fig. 2) are shown in Figs. 3 and 4, and comparison is made with the analytical ones [29]. It can be seen from Figs. 3 and 4 that the present results are in good agreement with the analytical solution. To study the convergent performance of the method, Table 1 provides the error percentage of stresses versus mesh density. In Table 1 α and β are defined by

$$\alpha = 100 \times (\boldsymbol{\sigma}_{rr(\text{exact})} - \boldsymbol{\sigma}_{rr(\text{present FE})})/\boldsymbol{\sigma}_{rr(\text{exact})}, \quad \beta = 100 \times (\boldsymbol{\sigma}_{\theta\theta(\text{exact})} - \boldsymbol{\sigma}_{\theta\theta(\text{present FE})})/\boldsymbol{\sigma}_{\theta\theta(\text{exact})} \tag{42}$$

and the stresses are calculated at radius $r = 0.15\,\text{m}$. In the course of computation, convergence was achieved with less than 9 iterations. It can be seen from the table that the results converge gradually to the analytical result when the mesh density is increased.

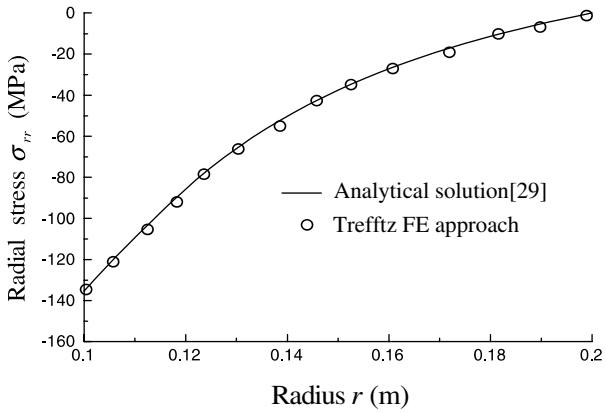

Fig. 4. Radial stress distributions for the thick cylinder along radius (mesh 2).

Table 1
Error coefficients α and β vary with Mesh density

Error coefficient	Mesh 1	Mesh 2	Mesh 3
α	3.72	2.83	1.73
β	2.51	1.92	1.08

Example 2. A 90° notched plane stress specimen under extension [30]. The finite element mesh used in the analysis is shown in Fig. 5. An elastic-perfectly plastic material is assumed and the von Mises yield criterion is used. The material constants of the notched specimen are $E = 7000\,\text{kgf/mm}^2$, $\nu = 0.2$, uniaxial yield stress $\sigma_s = 24.3\,\text{kgf/mm}^2$. Fig. 6 shows the applied load

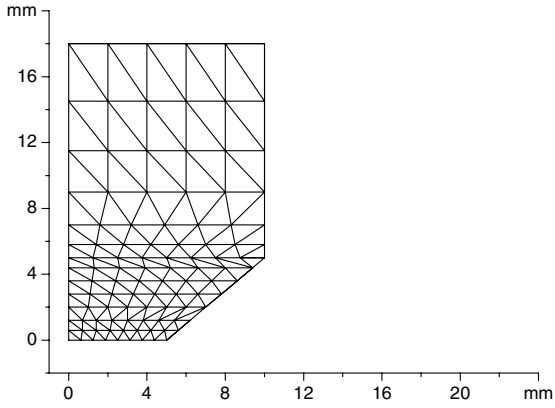

Fig. 5. Element mesh for notched specimen.

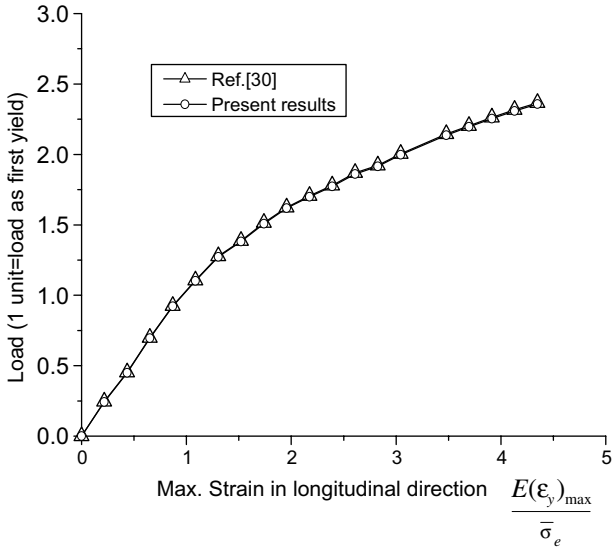

Fig. 6. Load–strain curve for 90° notched specimen.

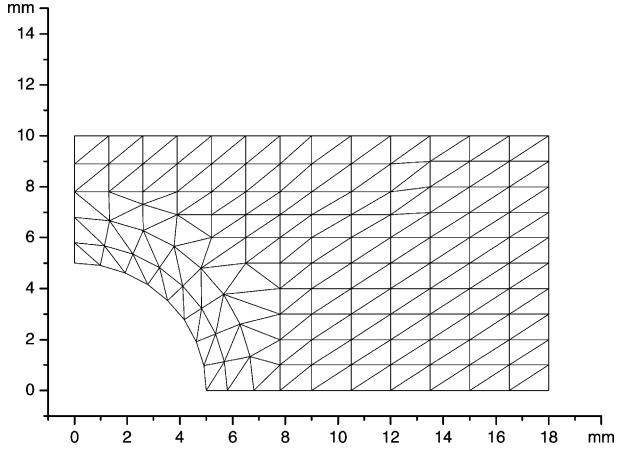

Fig. 7. Element mesh for the perforated plate.

versus maximum longitudinal strain. In order to allow for comparison with the results given in [30], the numerical results are plotted in a dimensionless form with one unit of load equal to the load at first yield and one unit of strain equal to the strain at yield of a uniform tensile specimen [30]. It can be seen from Fig. 6 that there is no difference between the two approaches within the plot accuracy. In the calculation, the loading increment is 0.1 unit and the convergence was achieved with less than 11 iterations.

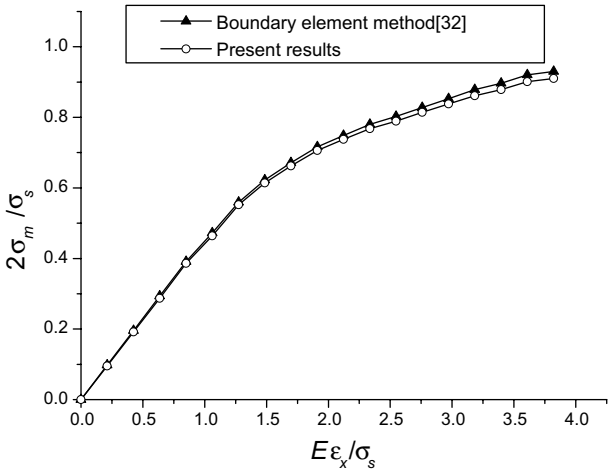

Fig. 8. Stress–strain curve at the root of the perforated plate.

Example 3. A perforated strip in axial tension under plane stress condition. This example was analyzed by using finite element method [31] and boundary element method [32]. A quadrant of the strip is modeled by 214 elements (Fig. 7) and Von Mises yield criterion is used in the calculation. The material constants used for the analysis are the same as those in Example 2, except for the linear hardening parameter $H = 224.0\,\mathrm{kgf/mm^2}$. The computed results of longitudinal strain coefficient $E\varepsilon_x/\sigma_s$ at the root of the plate versus dimensionless load factor $2\sigma_m/\sigma_s$, where $2\sigma_m = \sigma_x + \sigma_y$, are plotted in Fig. 8 and compared to the boundary element results. The maximum discrepancy of the results from the two methods is observed to be 2.16%. This discrepancy is acceptable.

8. Conclusions

A HT FE formulation for elastoplastic analysis of two-dimensional solids has been developed. In the analysis, a dual variational functional is constructed and used to derive HT FE formulation for the elastoplasticity of bulky solids. It should be mentioned that the modified variational functional in Qin [5] is limited to the case that nodes containing unknown displacements must connect with at least one inter-element boundary. This limitation has been removed by the proposed variational functional. Moreover, we use incremental field equations and have made a modification to the nonlinear boundary equation (9). The numerical results show that this modification is practicable.

Acknowledgment

This work was financially supported by the Australian Research Council. This support is gratefully acknowledged.

Appendix A. Incremental stress–strain relations

A.1. Isotropic hardening

In this theory it is assumed that during plastic flow the yield surface expands uniformly about the origin in the stress space maintaining its shape, centre and orientation. Following [27], we have

$$\dot{\boldsymbol{\sigma}}_{ij} = \dot{\boldsymbol{\sigma}}^{\mathrm{e}}_{ij} + \dot{\boldsymbol{\sigma}}^{\mathrm{p}}_{ij} \tag{A.1}$$

with

$$\dot{\boldsymbol{\sigma}}^{\mathrm{e}}_{ij} = \frac{E}{3(1-2v)}\dot{\varepsilon}_{ii}\delta_{ij} + 2G\dot{e}_{ij}, \tag{A.2}$$

$$\dot{\boldsymbol{\sigma}}^{\mathrm{p}}_{ij} = -\alpha^{*}\frac{2G\dfrac{\partial f}{\partial \boldsymbol{\sigma}_{kl}}\dot{\varepsilon}_{kl}}{\left(\dfrac{1}{2Gh} + \dfrac{\partial f}{\partial \boldsymbol{\sigma}_{pq}}\dfrac{\partial f}{\partial \boldsymbol{\sigma}_{pq}}\right)}\frac{\partial f}{\partial \boldsymbol{\sigma}_{kl}}, \tag{A.3}$$

where h is a positive definite function of $\boldsymbol{\sigma}_{ij}$, $\dot{e}_{ij} = \varepsilon_{ij} - \varepsilon_{ii}\delta_{ij}/3$, $f(f(\boldsymbol{\sigma}_{ij}) = \bar{\boldsymbol{\sigma}}_e)$ denotes yield function. The symbol α^* is defined by

$$\begin{aligned} &\alpha^{*} = 1 \quad \text{when } \bar{\boldsymbol{\sigma}}_e = c \text{ and } (\partial f/\partial \boldsymbol{\sigma}_{ij})\dot{\varepsilon}_{ij} \geqslant 0,\\ &\alpha^{*} = 0 \quad \text{when } \bar{\boldsymbol{\sigma}}_e < c \text{ or } \bar{\boldsymbol{\sigma}}_e = c \text{ and } (\partial f/\partial \boldsymbol{\sigma}_{ij})\dot{\varepsilon}_{ij} < 0, \end{aligned} \tag{A.4}$$

where the parameter c may be given as a function of the total plastic work [27]

$$c = F\left(\int \boldsymbol{\sigma}_{ij}\,\mathrm{d}\varepsilon^{\mathrm{p}}_{ij}\right). \tag{A.5}$$

The three functions f, h and F are related by $hF'(\partial f/\partial \boldsymbol{\sigma}_{ij})\boldsymbol{\sigma}_{ij} = 1$. Conversely, the incremental strain can be expressed by

$$\dot{\varepsilon}_{ij} = \dot{\varepsilon}^{\mathrm{e}}_{ij} + \dot{\varepsilon}^{\mathrm{p}}_{ij} \tag{A.6}$$

with

$$\dot{\varepsilon}^{\mathrm{e}}_{ij} = \frac{1-2v}{3E}\dot{\boldsymbol{\sigma}}_{ii}\delta_{ij} + \frac{\dot{S}_{ij}}{2G}, \tag{A.7}$$

$$\dot{\varepsilon}^{\mathrm{p}}_{ij} = \alpha^{**}h\frac{\partial f}{\partial \boldsymbol{\sigma}_{ij}}\dot{f}, \tag{A.8}$$

where

$$\begin{aligned} &\alpha^{**} = 1 \quad \text{when } \bar{\boldsymbol{\sigma}}_e = c \text{ and } \dot{f} \geqslant 0,\\ &\alpha^{**} = 1 \quad \text{when } \bar{\boldsymbol{\sigma}}_e < c \text{ or } \bar{\boldsymbol{\sigma}}_e = c \text{ and } \dot{f} < 0. \end{aligned} \tag{A.9}$$

A.2. The Prandtl–Reuss flow equation

In this special case, we have [27]

$$f = \bar{\boldsymbol{\sigma}}_e \tag{A.10a}$$

and Eq. (A.5) is replaced by

$$\bar{\boldsymbol{\sigma}}_e = H\left(\int \mathrm{d}\bar{\varepsilon}_{\mathrm{e}}^{\mathrm{p}}\right), \tag{A.10b}$$

where $\mathrm{d}\bar{\varepsilon}_{\mathrm{e}}^{\mathrm{p}} = (2\dot{\varepsilon}_{ij}^{\mathrm{p}}\dot{\varepsilon}_{ij}^{\mathrm{p}}/3)^{1/2}$, and H is a function which determined through relation $hH' = 1$. With this relation, the stress–strain relations (A.1) and (A.6) become

$$\dot{\boldsymbol{\sigma}}_{ij} = \frac{E}{3(1-2v)}\dot{\varepsilon}_{ii}\delta_{ij} + 2G\dot{e}_{ij} - \alpha^{*}\frac{2GS_{ij}S_{kl}\dot{\varepsilon}_{kl}}{\bar{\boldsymbol{\sigma}}_e\left(\frac{H'}{3G}+1\right)}, \tag{A.11}$$

$$\dot{\varepsilon}_{ij} = \frac{1-2v}{3E}\dot{\boldsymbol{\sigma}}_{ii}\delta_{ij} + \frac{\dot{S}_{ij}}{2G} + \alpha^{**}\frac{\partial 3S_{ij}\dot{\bar{\boldsymbol{\sigma}}}_e}{2\bar{\boldsymbol{\sigma}}_e H'} \tag{A.12}$$

for isotropic hardening material, and

$$\dot{\boldsymbol{\sigma}}_{ij} = \frac{E}{3(1-2v)}\dot{\varepsilon}_{ii}\delta_{ij} + 2G\dot{e}_{ij} - \alpha^{*}\frac{3GS_{ij}S_{kl}\dot{\varepsilon}_{kl}}{k^2}, \tag{A.13}$$

$$\dot{\varepsilon}_{ij} = \frac{1-2v}{3E}\dot{\boldsymbol{\sigma}}_{ii}\delta_{ij} + \frac{\dot{S}_{ij}}{2G} + \alpha^{**}\dot{\lambda}S_{ij} \tag{A.14}$$

for perfectly plastic material, where $\bar{\boldsymbol{\sigma}}_e = (3S_{ij}S_{ij}/2)^{1/2}$, k is a material constant defined in the yield condition

$$S_{ij}S_{ij} = 2k^2 \tag{A.15}$$

and $\dot{\lambda}$ is determined by

$$\dot{\lambda} = \lim_{\dot{\bar{\boldsymbol{\sigma}}}_e \to 0, H' \to 0} \frac{3\dot{\bar{\boldsymbol{\sigma}}}_e}{2\bar{\boldsymbol{\sigma}}_e H'} > 0. \tag{A.16}$$

References

[1] J. Jirousek, N. Leon, A powerful finite element for plate bending, Comp. Meth. Appl. Mech. Eng. 12 (1977) 77–96.
[2] J. Jirousek, Basis for development of large finite elements locally satisfying all field equations, Comp. Meth. Appl. Mech. Eng. 14 (1978) 65–92.
[3] E. Trefftz, Ein Gegenstück zum Ritzschen Verfahren, in: Proc. 2nd Int. Congr. of Applied Mechanics, Zurich, 1926, pp. 131–137.

[4] J. Jirousek, A. Wroblewski, T-elements: state of the art and future trends, Arch. Comput. Meth. Eng. 3 (1996) 323–434.
[5] Q.H. Qin, The Trefftz Finite and Boundary Element Method, WIT Press, Southampton, 2000.
[6] J. Jirousek, A. Venkatesh, Hybrid-Trefftz plane elasticity elements with *p*-method capabilities, Int. J. Numer. Meth. Eng. 35 (1992) 1443–1472.
[7] J. Jirousek, L. Guex, The hybrid-Trefftz finite element model and its application to plate bending, Int. J. Numer. Meth. Eng. 23 (1986) 651–693.
[8] Q.H. Qin, Hybrid Trefftz finite element approach for plate bending on an elastic foundation, Appl. Math. Model. 18 (1994) 334–339.
[9] Q.H. Qin, Hybrid Trefftz finite element method for Reissner plates on an elastic foundation, Comp. Meth. Appl. Mech. Eng. 122 (1995) 379–392.
[10] R. Piltner, A quadrilateral hybrid-Trefftz plate bending element for the inclusion of warping based on a three-dimensional plate formulation, Int. J. Numer. Meth. Eng. 33 (1992) 387–408.
[11] R. Piltner, On the representation of three-dimensional elasticity solutions with the aid of complex value functions, J. Elasticity 22 (1989) 45–55.
[12] Wroblewski A., A.P. Zielinski, J. Jirousek, Hybrid-Trefftz *p*-element for 3-D axisymmetric problems of elasticity, in: C. Hirsch, O.C. Zienkiewicz, E. Oñate (Eds.), Numerical Methods in Engineering'92, Proc. First Eur. Conf. on Numerical Methods in Engineering, Brussel, Elsevier, Amsterdam, 1992, pp. 803–810.
[13] A.P. Zielinski, O.C. Zienkiewicz, Generalized finite element analysis with T-complete boundary solution functions, Int. J. Numer. Meth. Eng. 21 (1985) 509–528.
[14] M. Stojek, Least-squares Trefftz-type elements for the Helmholtz equation, Int. J. Numer. Meth. Eng. 41 (1998) 831–849.
[15] G.M. Vörös, J. Jirousek, Application of the hybrid-Trefftz finite element model to thin shell analysis, in: P. Ladeveze, O.C. Zienkiewicz (Eds.), Proc. Eur. Conf. on New Advances in Comput. Struct. Mech., Giens, France, Elsevier, Amsterdam, 1991, pp. 547–554.
[16] J.A.T. Freitas, Hybrid-Trefftz displacement and stress elements for elasto-dynamic analysis in the frequency domain, Comput. Assist. Mech. Eng. Sci. 4 (1997) 345–368.
[17] Q.H. Qin, Transient plate bending analysis by hybrid Trefftz element approach, Commun. Numer. Meth. Eng. 12 (1996) 609–616.
[18] J. Jirousek, Q.H. Qin, Application of hybrid-Trefftz element approach to transient heat conduction analysis, Comput. Struct. 58 (1996) 195–201.
[19] Q.H. Qin, Postbuckling analysis of thin plates by a hybrid Trefftz finite element method. Comp, Meth. Appl. Mech. Eng. 128 (1995) 123–136.
[20] A.P. Zielinski, Trefftz method: elastic and elastoplastic problems, Comput. Meth. Appl. Mech. Eng. 69 (1998) 185–204.
[21] J.A.T. Freitas, Z.M. Wang, Hybrid-Trefftz stress elements for elastoplasticity, Int. J. Numer. Meth. Eng. 43 (1998) 655–683.
[22] P.K. Banerjee, D.N. Cathie, T.G. Davies, Two- and three-dimensional problems of elasto-plasticity, in: P.K. Banerjee, R. Butterfield (Eds.), Developments in Boundary Element Methods—1, Applied Science Publishers, London, 1979, pp. 65–95.
[23] R. Piltner, Special finite elements with holes and internal cracks, Int. J. Numer. Meth. Eng. 21 (1985) 1471–1485.
[24] J. Jirousek, Variational formulation of two complementary hybrid-Trefftz FE models, Commun. Numer. Meth. Eng. 9 (1993) 837–845.
[25] J. Jirousek, A.P. Zielinski, Dual hybrid-Trefftz element formulation based on independent boundary traction frame, Int. J. Numer. Meth. Eng. 36 (1993) 2955–2980.
[26] H.C. Simpson, S.J. Spector, On the positivity of the second variation of finite elasticity, Arch. Rational Mech. Anal. 98 (1987) 1–30.
[27] K. Washizu, Variational Methods in Elasticity & Plasticity, third ed., Pergamon Press, Oxford, 1982.
[28] Q.H. Qin, Y.Y. Huang, BEM of postbuckling analysis of thin plates, Appl. Math. Model. 14 (1990) 544–548.
[29] P.G. Hodge, G.N. White, A quantitative comparison of flow and deformation theories of plasticity, J. Appl. Mech. 17 (1950) 180–184.

[30] P.V. Marcal, I.P. King, Elastic–plastic analysis of two-dimensional stress systems by the finite element method, Int. J. Mech. Sci. 9 (1967) 143–155.
[31] G.C. Nayak, O.C. Zienkiewicz, Elasto-plastic stress analysis generalization for various constitutive relations including strain softening, Int. J. Numer. Meth. Eng. 5 (1972) 113–135.
[32] P.K. Banerjee, S.T. Raveendra, Advanced boundary element analysis of two- and three-dimensional problems of elasto-plasticity, Int. J. Numer. Meth. Eng. 23 (1986) 985–1002.